

Design and Simulation of 3D Printed Check Valves Using Fluid-Structure Interaction

Alexa M. Melvin^{*1}, Thomas J. Roussel¹

¹Department of Bioengineering, University of Louisville, Louisville, KY, USA

^{*}Corresponding Author: alexa.melvin@louisville.edu

Abstract: Passive, one-way valves, also known as check valves, while common at the macro scale, are an essential microfluidic feature that facilitates flow rectification. These structures are commonly used in micropump configurations to control flow. Check valves have numerous applications within microfluidics with the large majority being fabricated by replica molding. There has been a shift towards 3D printing microfluidics to reduce the time and cost associated with developing prototypes. Only a handful of studies have developed microvalves using stereolithography (SLA). However, fused deposition modeling (FDM) printers are more widely available and cost effective compared to SLA. This study focused on analyzing the range of valve thicknesses necessary to promote forward flow using commonly available FDM filaments. An arbitrary Lagrangian-Eulerian model, a form of fluid-structure interaction (FSI), was set-up in COMSOL Multiphysics 4.2a. Five 3D printer filament materials were compared in simulations of valve deformation over a 0.75 second transient period using the material properties of PDMS as a baseline. The maximum valve deflection for ABS, nylon, PETG, PLA, and TPU was 3.34, 3.08, 3.37, 3.00, and 6.45 μm , respectively. The simulation resulted in a maximum valve deformation of 6.65 μm for PDMS. As expected, materials with a Young's modulus close to PDMS allows valve structures to actuate with adequate forward flow.

Keywords: microvalves, droplet control, Fluid-Structure Interaction, 3D printing

1. Introduction

Passive, one-way valves (check valves) are an essential microfluidic component that facilitates flow rectification. They also control timing, routing, and separation of fluids. These structures are commonly used in reciprocating micropump configurations to control flow by exerting pressure forces on the working fluid [1]. Their operation can be compared to a traditional diode in electronics where the flow of current can flow in only one direction (analogous to volumetric flow), but only after a small forward voltage is applied (analogous to pressure). The valve is opened when the upstream pressure is of a sufficient magnitude to overcome the combination of

downstream (back) pressure and any restoring force [2] which is typically present due to internal stresses created by deformation of the valve body or structure. Check valves have numerous applications within microfluidics such as gas flow control [3], [4], and integrated into pumps [5]–[7], and in connection with chemical analysis systems [8], [9].

A large majority of microfluidic valves reported in the literature are fabricated by replica molding using polydimethylsiloxane (PDMS). PDMS is poured onto master molds and placed in an oven to cure. After hardening, the PDMS is removed from the mold and must undergo an adhesion process (typically oxygen plasma bonding) to enclose the channels. PDMS has become a popular research tool as it is inexpensive, biocompatible, and translucent. However, PDMS devices are difficult to scale up and commercialize as they are labor intensive, primarily due to the master mold creation [10].

3D printing has emerged as a fabrication technique that offers interesting flexibility in the development of custom and unique microfluidic structures [11]. As with other uses of this rapid prototyping technology, R&D efforts can be greatly accelerated due to drastic reductions in time and cost expenditures. The most common 3D printing technique, fused deposition modeling (FDM), operates by heating thermoplastic materials precisely to a specified melting point. The material is then extruded (typically through a sub-millimeter orifice/nozzle; 500 μm is common) layer by layer to create a 3D object. FDM has been widely used in research due to ease of use and the availability of inexpensive benchtop, consumer-grade equipment and ease of use. Many of the software programs used with the printers are open-source and therefore ripe for customization.

Stereolithography (SLA), an alternative 3D printing technology, has recently become of great interest to researchers. Quasi-arbitrary 3D shapes are formed from a liquid photoresin precursor and an accurately and precisely focused beam of light that cures the resin through photopolymerization. SLA can simplify the pathway to commercialization and is amenable to printing structures directly generated after simulation via finite element modeling [12]. The small geometric features attainable with SLA lends itself

well to the development of extremely complicated 3D microfluidic manifolds [13], [14].

Interestingly, only a handful of studies have described the development of microvalves using SLA [15], [16]. However, SLA desktop units are less common and more expensive than FDM, perhaps simply due to availability, but this is changing as the technology matures and equipment prices drop. To the best of our knowledge, no studies have attempted to design and print microvalves using more common FDM printers. This study was performed to analyze the range of valve thicknesses necessary to promote forward flow using commonly available 3D printer filament materials.

2. Fluid-Structure Interaction: Governing Equations and Theory

The field of computational fluid dynamics (CFD) utilizes data structures and numerical analysis to solve and analyze problems dealing with fluid flow. The equations for almost all CFD problems utilize the Navier-Stokes relationships that were derived from the fundamental principles of conservation of mass, momentum, and energy, as applied to single-phase fluid flows. The small dimensions of microchannels lead to a Reynold's number that is usually less than 100, ensuring the flow remains laminar (turbulent flow begins with a Reynold's number of approximately 2000) [17]. Reynolds number is determined by

$$Re = \frac{\rho v l}{\mu}$$

Where μ is the viscosity, ρ is the density, l is the characteristic length, and v is the velocity.

Fluid-structure interaction (FSI) can be described as a multiphysics coupling between fluid dynamics and structural mechanics. When fluid flow encounters a structure, forces (stress and strain) that can lead to deformation are exerted on the object. The model in this study utilizes an Arbitrary Lagrangian-Eulerian (ALE) formulation. The Eulerian framework is used for the fluid, while the Lagrangian framework is for the translating solid (valve). By using the ALE formulation, the solid moving mesh is used to track the deformation of the fluid mesh. In ALE, the nodes in the mesh can be moved in a normal Lagrangian fashion or fixed in a Eulerian manner. This allows the mesh to move in an arbitrary fashion to give a continuous rezoning capability. Greater distortions of the mesh can be achieved with ALE than with the standard Lagrangian method [18].

A report is generated from the COMSOL Multiphysics software that includes the geometric dimensions, equations, variables, and results. All governing equations used for the ALE simulations were extracted from a sample report and are highlighted below. The structural mechanics solver uses a linear elastic material model. The deformation is described by:

$$\rho \frac{\partial^2 u}{\partial t^2} - \nabla \cdot \sigma = Fv \quad \text{Eq. 1}$$

where σ is calculated by

$$\sigma = \int^1 F S F^T \quad \text{Eq. 2}$$

and F is calculated by

$$F = (I + \nabla u). \quad \text{Eq. 3}$$

The total strain tensor in terms of the displacement gradient is described as:

$$\varepsilon = \frac{1}{2} [(\nabla u)^T + \nabla u + (\nabla u)^T \nabla u] \quad \text{Eq. 4}$$

where ∇u is the displacement gradient and ε is the total strain tensor.

The fluid flow is described by single-phase, incompressible Navier-Stokes equations:

$$\rho \frac{\partial u}{\partial t} + \rho(u \cdot \nabla)u = \nabla \cdot [-\rho I + \mu(\nabla u + (\nabla u)^T)] + F \quad \text{Eq. 5}$$

$$\rho \nabla \cdot u = 0 \quad \text{Eq. 6}$$

where u denotes the velocity (m/s), μ is the viscosity (Pa·s), ρ is the density (kg/m³), T is the absolute temperature (K), and t is time (s). The Navier-Stokes equations are solved on a freely moving mesh domain (the fluid domain). The mesh deformation relative to its initial shape is computed using hyperelastic smoothing. This looks for the minimum mesh deformation energy inspired by neo-Hookean (hyperelastic) materials:

$$W = \int \frac{\mu}{2} (I_1 - 3) + \frac{\kappa}{2} (j - 1)^2 dV \quad \text{Eq. 7}$$

where μ and κ are shear and bulk moduli, respectively. The invariants (J and I_1) are given by:

$$J = \det(\nabla x^x) \quad \text{Eq. 8}$$

$$I_1 = J^{-2/3} \text{tr}((\nabla x^x)^T \nabla x^x) \quad \text{Eq. 9}$$

Hyperelastic smoothing is nonlinear and robust resulting in a smoother result especially in areas where the mesh is stretched.

A no-slip (zero velocity) boundary condition is applied to all interior walls. For fluid flow, the inlet boundary condition assumes normal inflow velocity perpendicular to the face of the flow inlet:

$$u = -u_0 n \quad \text{Eq. 10}$$

where u_0 is the inlet velocity and n is the normal vector to the FSI boundary.

The boundary condition at the outlet assumes that the total pressure is equal to zero:

$$p = p_0 \quad \text{Eq. 11}$$

$$[\mu(\nabla u + (\nabla u)^T)]n = 0 \quad \text{Eq. 12}$$

The structural velocity of the valve is transmitted to the fluid at the fluid-solid boundary. In turn, the fluid flow stresses act as a loading on the inner boundary of the solid wall (valve). The boundary conditions for the fluid-structure interface are described by the following equations:

$$u_{fluid} = u_{valve} \quad \text{Eq. 13}$$

$$u_{valve} = \frac{\partial u_{solid}}{\partial t} \quad \text{Eq. 14}$$

$$\sigma \cdot n = \Gamma \cdot n \quad \text{Eq. 15}$$

and Γ is calculated using

$$\Gamma = [-\rho I + \mu(\nabla u_{fluid} + (\nabla u_{fluid})^T)] \quad \text{Eq. 16}$$

where u_{valve} and u_{fluid} are the velocity vector of the valve and fluid, n is the normal vector to the FSI boundary, and σ (Γ) is the stress tensor.

3. Microvalve Set-Up in COMSOL Multiphysics®

Two-dimensional representations of a variety of designs were created in COMSOL Multiphysics® v.4.2 (**Figure 1**). The linear elastic model was assigned to the valve, while the rest of the geometry was classified as a laminar flow region. The two physics were fully coupled using the FSI module. A monolithic approach was used allowing both solid and liquid equations to be formulated and solved at the same time. The velocity of the fluid was set so laminar flow characteristics were fully developed when it entered the channel. The inlet velocity was calculated as

$$v_i = u_{mean} \times 6 \times (H - Y) \times \frac{Y}{H^2} \quad \text{Eq. 17}$$

and u_{mean} was calculated using

$$u_{mean} = \frac{U \times t^2}{\sqrt{t^4 - 0.07t^2 + 0.0016}} \quad \text{Eq. 18}$$

where H is the height of the channel, Y is length of the channel, u_{mean} is the centerline velocity, t is time, and U is the inlet velocity.

In the example design (shown in Figure 1), the channel was 100 μm high and 300 μm wide. The restriction, or valve stop, is 25 μm wide and 55 μm high. The valve (outlined in green) is 57.5 μm high. The valve width was manually increased iteratively until there was not enough deflection for forward flow to occur at a fixed flow rate.

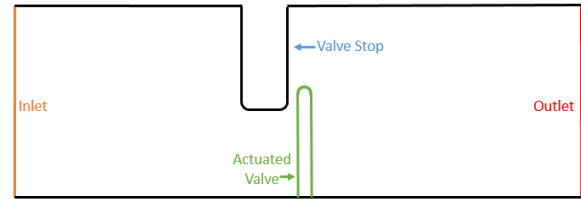


Figure 1. 2D representation of check valve geometry to prevent backflow

The material properties of five commonly available 3D printer filaments were used in the simulations: polylactic acid (PLA), acrylonitrile butadiene styrene (ABS), nylon, polyethylene terephthalate glycol (PETG), and thermoplastic polyurethane (TPU). Valve performance using the material properties of PDMS was also simulated and the results were used as a baseline reference. The properties of these materials can be found in **Table 1**. A 3D model with the same geometric design was tested to verify the accuracy of the 2D configuration. The two-dimensional design was extended to create a depth of 100 μm . The valve spanned the entire depth of the channel, with only the base geometrically fixed in space.

Table 1. Properties of tested materials

Material	ρ (kg/m ³)	ν	E (Pa)
PLA	1250	0.33	3.5×10^9
ABS	1100	0.35	2.05×10^9
Nylon	1130	0.39	2.95×10^9
PETG	1260	0.40	2.0×10^9
TPU	1100	0.40	4.5×10^6
PDMS	0.97	0.40	0.87×10^6

4. Results and Discussion

The simulation was configured to analyze valve deformation for six different materials from 0 to 0.75 seconds (when steady state occurred for the most flexible material). **Figure 2** shows the von Mises stress and surface velocity magnitude for the initial valve

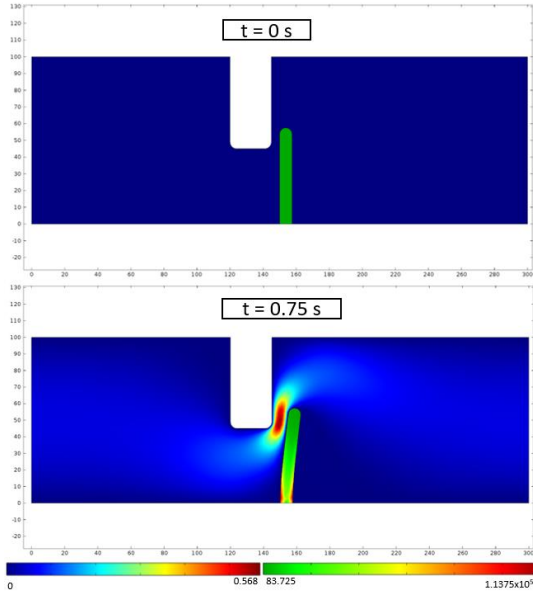


Figure 2. Surface von Mises Stress and surface velocity magnitude for the valve initial position (top) and valve is completely open (bottom) for a TPU valve with a width of 7.5 μm.

position ($t = 0$ s) and the steady state position of the valve ($t = 0.75$ s). When the valve is “closed”, fluid was allowed to leak through the 5 μm gap.

Figure 3 shows the mesh velocity and the von Mises stress of the valve. When the fluid forces come in contact with the valve, the forces are transferred to the solid causing it to deform rapidly. After the initial deflection, the valve bounces back slightly (negative velocity) before reaching its steady-state open position.

The material properties, specifically the Young’s modulus, play a major role in the magnitude of valve deflection (**Figure 4**). **Figure 5** shows valve deformations for four of the 3D printer filament materials. A 2D cut point was placed on the edge of the valve (closest to the outlet) to measure the solid deformation and mesh velocity. ABS and PETG followed the same deformation patterns and had slightly higher deformations than PLA and nylon. However, all of these filaments require extremely thin valves (less than 4 μm thick) to allow enough deflection to promote forward flow. This is due to the high Young’s modulus of these materials, which are 2000 to 4000 times greater compared to PDMS. A significant increase in velocity (greater than 4 times) would be required to actuate the thicker valves.

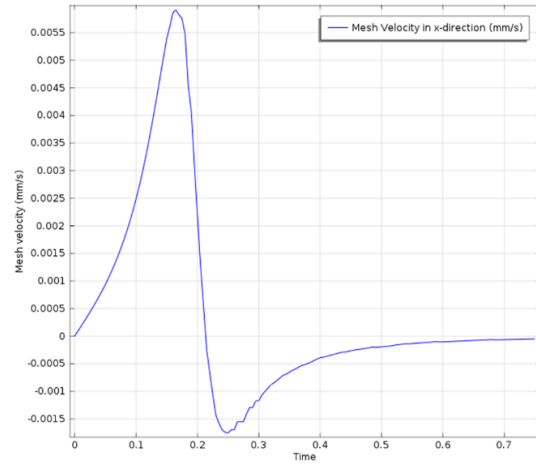


Figure 3. Solid deformation velocity profile

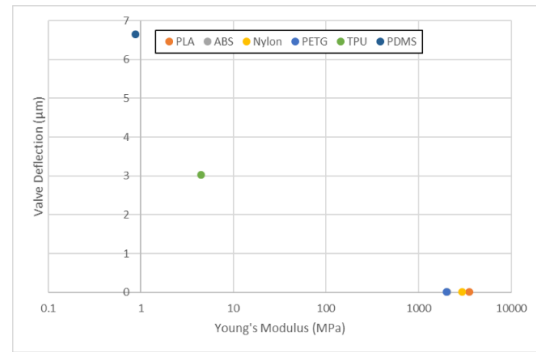


Figure 4. Comparison of valve deformation for a 12 μm width valve for the six different materials (log scale used on the x-axis to help differentiate PDMS and TPU)

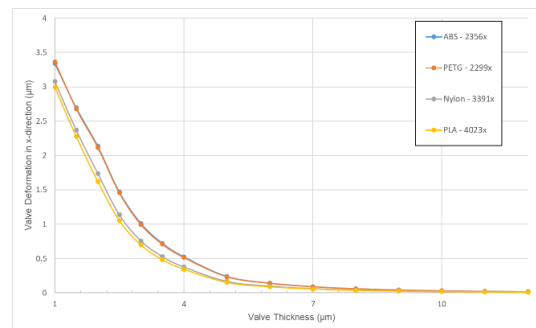


Figure 5. Valve deformation of four 3D printer filaments. Note that ABS and PETG follow the same trend and overlap.

A comparison of the valve deformations of TPU and PDMS are shown in **Figure 6**. TPU has a Young's modulus similar to PDMS and followed the same deformation trend. However, TPU required narrower valve thicknesses (compared to PDMS) due to its roughly five times greater Young's modulus. TPU has several advantages such as resistance to abrasion, elasticity, and mechanical properties similar to rubber. It is commonly used in wet environments to resist oil and hydrocarbons making it a viable option for microfluidics.

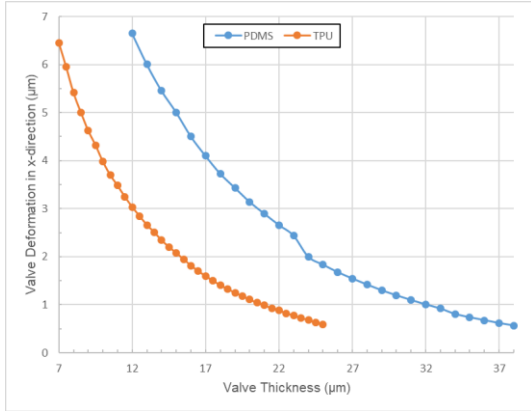


Figure 6. Valve deformation of TPU and PDMS

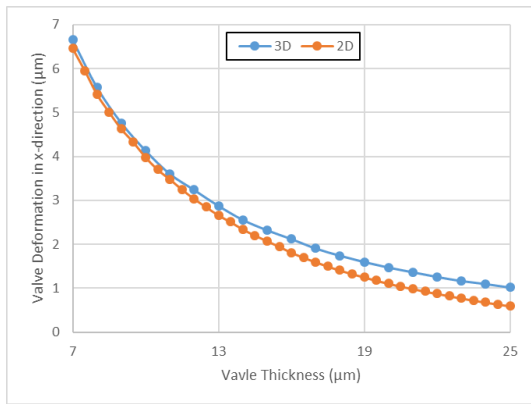


Figure 7. Comparison of TPU valve deformation in 2D and 3D simulations

A 3D model was designed and tested in COMSOL to verify the results of the 2D simulations. Since the 3D simulations are more memory intensive and time-consuming, only the TPU valve was simulated.

Figure 7 compares the 2D and 3D simulations of the TPU valves. The 3D simulations had slightly larger deflections, but still closely followed the trend of the 2D simulations. As the valve thickness increase, the

Table 2. Comparison of the TPU valve deformation with their associated percent difference. Note the large percent differences can be attributed to the element mesh size. More accurate results could be obtained by using the extremely fine mesh for both models.

Valve Thickness (μm)	2D (μm)	3D (μm)	Percent Difference
7	6.45	6.65	2.99
8	5.41	5.57	2.84
9	4.63	4.76	2.95
10	3.98	4.13	3.76
11	3.48	3.60	3.47
12	3.03	3.24	6.51
13	2.66	2.88	7.79
14	2.34	2.56	8.86
15	2.08	2.32	11.16
16	1.81	2.12	15.68
17	1.60	1.91	17.62
18	1.41	1.74	21.30
19	1.25	1.60	24.32
20	1.11	1.47	28.40
21	0.99	1.37	32.34
22	0.88	1.26	35.73
23	0.77	1.17	40.83
24	0.68	1.10	47.20
25	0.60	1.02	52.36

percent difference between the 2D and 3D simulations increase (**Table 2**).

5. Conclusions

Materials with sufficiently low Young's modulus, such as TPU, were shown to allow adequate actuation of the valve at the specified flow rate to allow forward flow. TPU exhibited similar deformation when directly compared to PDMS demonstrating the potential use of FDM filaments for microvalves. Future studies include the optimization of check valve geometry to realizable 3D printed features and custom geometric shapes to prevent backflow. Future studies will evaluate the minimum flow rates required to open the check valves for a variety of designs including interdigitated arrays and tapered structures. Lastly, advanced 3D structures, such as a biomimetic leaflet valve, will be investigated.

References

- [1] D. J. Laser and J. G. Santiago, "A review of micropumps," *J. Mech. Des. Trans. ASME*, no. 14, pp. R35–R64, 2004.

- [2] A. K. Au, H. Lai, B. R. Utela, and A. Folch, "Microvalves and Micropumps for BioMEMS," *Micromachines*, pp. 179–220, 2011.
- [3] J. H. Jerman, "Electrically-activated, micromachined diaphragm valves," in *Micro System Technologies 90*, Springer, 1990, pp. 806–811.
- [4] J. Tiren, L. Tenerz, and B. Hök, "A batch-fabricated non-reverse valve with cantilever beam manufactured by micromachining of silicon," *Sensors and Actuators*, vol. 18, no. 3–4, pp. 389–396, 1989.
- [5] F. C. M. Van De Pol, D. G. J. Wonnink, M. Elwenspoek, and J. H. J. Fluitman, "A thermo-pneumatic actuation principle for a microminiature pump and other micromechanical devices," *Sensors and Actuators*, vol. 17, no. 1–2, pp. 139–143, 1989.
- [6] L. Smith and B. Hok, "A silicon self-aligned non-reverse valve," in *Solid-State Sensors and Actuators, 1991. Digest of Technical Papers, TRANSDUCERS '91., 1991 International Conference on*, 1991, pp. 1049–1051.
- [7] R. Zengerle, A. Richter, and H. Sandmaier, "A micro membrane pump with electrostatic actuation," in *Micro Electro Mechanical Systems, 1992, MEMS '92, Proceedings. An Investigation of Micro Structures, Sensors, Actuators, Machines and Robot. IEEE*, 1992, pp. 19–24.
- [8] S. Shoji, M. Esashi, and T. Matsuo, "Prototype miniature blood gas analyser fabricated on a silicon wafer," *Sensors and Actuators*, vol. 14, no. 2, pp. 101–107, 1988.
- [9] S. Nakagawa, S. Shoji, and M. Esashi, "A micro chemical analyzing system integrated on a silicon wafer," in *Micro Electro Mechanical Systems, 1990. Proceedings, An Investigation of Micro Structures, Sensors, Actuators, Machines and Robots. IEEE*, 1990, pp. 89–94.
- [10] A. Folch, *Introduction to bioMEMS*. CRC Press, 2016.
- [11] A. K. Au, W. Huynh, L. F. Horowitz, and A. Folch, "3D-Printed Microfluidics," *Angew. Chemie - Int. Ed.*, vol. 55, no. 12, pp. 3862–3881, 2016.
- [12] A. K. Au, W. Lee, and A. Folch, "Mail-Order Microfluidics: Evaluation of Stereolithography for the Production of Microfluidic Devices," *Lab Chip*, vol. 7, pp. 1294–1301, 2014.
- [13] A. Bertsch, S. Heimgartner, P. Cousseau, and P. Renaud, "Static micromixers based on large-scale industrial mixer geometry," *Lab Chip*, vol. 1, no. 1, pp. 56–60, 2001.
- [14] B. Kaehr and J. B. Shear, "High-throughput design of microfluidics based on directed bacterial motility," *Lab Chip*, vol. 9, no. 18, pp. 2632–2637, 2009.
- [15] Y. S. Lee, N. Bhattacharjee, and A. Folch, "3D-printed Quake-style microvalves and micropumps," *Lab Chip*, vol. 18, no. 8, pp. 1207–1214, 2018.
- [16] A. K. Au, N. Bhattacharjee, L. F. Horowitz, T. C. Chang, and A. Folch, "3D-Printed Microfluidic Automation," *Lab Chip*, no. 207890, pp. 531–540, 2015.
- [17] B. J. Kirby, *Micro-and nanoscale fluid mechanics: transport in microfluidic devices*. Cambridge university press, 2010.
- [18] J. Donea, A. Huerta, J. Ponthot, and A. Rodr, "Arbitrary Lagrangian – Eulerian Methods," *Encycl. Comput. Mech.*, pp. 1–25, 1999.